

Optical-phonon behavior in $Zn_{1-x}Mn_xSe$: Zinc-blende and wurtzite structures

P. D. Lao and Yile Guo

Department of Physics, Fudan University, Shanghai 200433, People's Republic of China

G. G. Siu

Department of Applied Science, City Polytechnic of Hong Kong, Kowloon, Hong Kong

S. C. Shen

National Laboratory for Infrared Physics, Shanghai Institute of Technical Physics, Academia Sinica, Shanghai 200083, People's Republic of China

(Received 4 June 1993)

Optical phonons of mixed-crystal $Zn_{1-x}Mn_xSe$ in both zinc-blende and wurtzite structures are investigated by Raman scattering. A calculation of the compositional dependence of the optical-phonon frequency in $Zn_{1-x}Mn_xSe$ is performed using a modified random-element isodisplacement model with some detailed consideration. It confirms that $Zn_{1-x}Mn_xSe$ shows an intermediate-mode behavior. The constant Θ which describes the effect of variation of the lattice parameter on the force constants should be different for individual mixed crystals. The phonon-mode splitting in wurtzite-structure $Zn_{1-x}Mn_xSe$ is mainly attributed to the directional dependence of the force constants.

The vibrational spectra of diluted magnetic semiconductors (DMS), mixed crystals of tetrahedrally coordinated II-VI semiconductors where a fraction of the cations is replaced by a magnetic element such as Mn^{2+} , are of special interest in view of the fundamental aspects of lattice vibrations. Like other semiconductor alloys, the zone-center optical phonons in DMS show a variety of patterns for their mode behavior: they exhibit "one-mode," "two-mode," or "intermediate-mode" behavior depending on the vibrational characteristics of the end members. For example, optical phonons in $Zn_{1-x}Mn_xS$ (Ref. 1) exhibit one-mode behavior, those in $Cd_{1-x}Mn_xTe$ (Ref. 2) and $Cd_{1-x}Mn_xSe$ (Ref. 3) exhibit two-mode behavior, while $Zn_{1-x}Mn_xTe$ (Ref. 4) shows an interesting intermediate-mode behavior.

Many studies of the diluted magnetic semiconductor $Zn_{1-x}Mn_xSe$ have already been done on its strong exchange interaction between band electrons and the localized electrons of Mn^{2+} , as well as lattice parameter and optical absorption. However, investigation on its lattice vibration behavior is far less complete. It is known that $Zn_{1-x}Mn_xSe$ is zinc blende for $0 \leq x \leq 0.3$ and wurtzite for $0.33 \leq x \leq 0.57$.⁵ Studies on the phonons of $Zn_{1-x}Mn_xSe$ up to now are all within the range of $0 \leq x \leq 0.33$ and the results are inconsistent. Arora *et al.*⁶ inferred from their Raman-scattering measurement that the zone-center optical phonons of zinc-blende $Zn_{1-x}Mn_xSe$ exhibit an intermediate-mode behavior. Lu *et al.*^{7,8} concluded from their far-infrared reflection measurement that the $x=0.18$ sample shows a two-mode behavior while the $x=0.31$ sample seems to be in an intermediate state of two-mode as well as one-mode behavior.

In this paper, we extend the scope of studies on the optical phonons of $Zn_{1-x}Mn_xSe$ from zinc-blende structure

to wurtzite structure. We present our Raman-scattering data of its optical phonons for material with x in the range 0.3–0.5 and the calculation of the phonon frequency as a function of composition by modified random-element isodisplacement (MREI) model with some detailed considerations to fit the measured data.

EXPERIMENT

The samples used in this study were grown by the modified Bridgman method. Their compositions are $x=0.3, 0.4, 0.5$, respectively. Raman spectra were recorded at room temperature in backscattering configuration, with an excitation power 20 mW of the 5145-Å Ar^+ laser line. The slit of the double monochromator was set at 400 μm .

RESULTS AND DISCUSSION

The room-temperature Raman spectrum of the sample of $Zn_{0.5}Mn_{0.5}Se$ is shown in Fig. 1. The frequencies of the optical-phonon modes of $Zn_{1-x}Mn_xSe$ are plotted in Fig. 2 (left side) as a function of composition. The symbol \circ stands for our results, while $+$ is the data from Arora *et al.*⁶ As illustrated in this figure, the optical-phonon frequencies obtained in the two studies near $x=0.3$ do not agree.

This is even more evident if the result of Lu *et al.*⁸ is included. This is possibly due to the structural phase transition from zinc blende to wurtzite near $x=0.3$, and the samples studied with composition near phase transition may either be zinc blende or wurtzite or the mixture of the two structures.

Several models have been proposed to describe the optical-phonon behavior of the mixed crystal. The popular one is random-element isodisplacement (REI) model.⁹

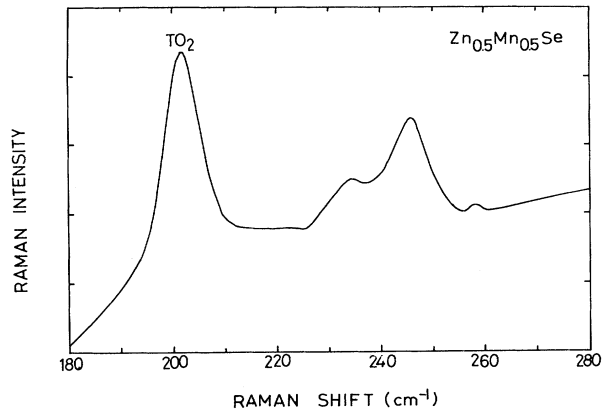


FIG. 1. Room-temperature Raman spectrum of wurtzite $\text{Zn}_{0.5}\text{Mn}_{0.5}\text{Se}$.

The fundamental assumptions of the REI model¹⁰ are that in the long-wavelength limit ($q \sim 0$), the anions, and the cations of similar species vibrate with the same phase and amplitude, and the force which each ion experiences is provided by a statistical average of the interaction with its neighbors. The model was modified by Genzel, Martin, and Perry¹¹ with the emphasis on the use of local fields and complete determination of phonon frequency by the macroscopic parameters of the pure end members. Peterson's work⁴ followed this philosophy and, furthermore, combined $\text{Cd}_{1-x}\text{Mn}_x\text{Te}$ and $\text{Zn}_{1-x}\text{Mn}_x\text{Te}$ to calculate compositional dependence of their phonon frequencies together. This allows one to incorporate second-neighbor force constants and a linear dependence of the force constants on the lattice parameter into the model without resorting to microscopic fitting parameters.

At first we follow Peterson's method, i.e., combine $\text{Cd}_{1-x}\text{Mn}_x\text{Se}$ and $\text{Zn}_{1-x}\text{Mn}_x\text{Se}$ to calculate their phonon frequencies as a function of composition. As an initial approximation we neglect the difference between zinc-blende and wurtzite structure of $\text{Zn}_{1-x}\text{Mn}_x\text{Se}$. The parameters used in calculation are listed in Table I, in which $\omega_I(\text{MnSe:Zn})$ and $\omega_I(\text{ZnSe:Mn})$ are fitting parameters

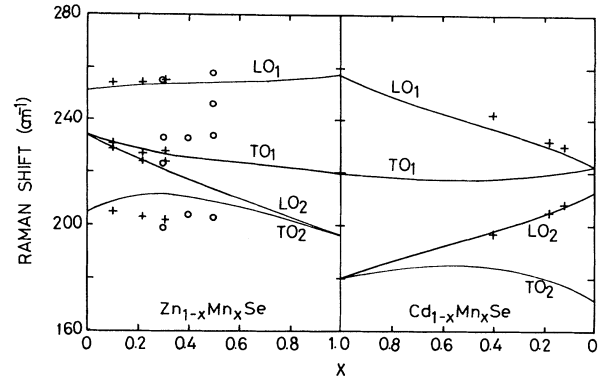


FIG. 2. The frequencies of the $\text{Cd}_{1-x}\text{Mn}_x\text{Se}$ and $\text{Zn}_{1-x}\text{Mn}_x\text{Se}$ zone-center optical phonons. The curves were generated using the MREI model assuming same value of θ for $\text{Cd}_{1-x}\text{Mn}_x\text{Se}$ and $\text{Zn}_{1-x}\text{Mn}_x\text{Se}$.

ters and marked with an asterisk. The curves generated are illustrated in Fig. 2. It can be seen that the curves apparently deviate from the experimental data, both in $\text{Zn}_{1-x}\text{Mn}_x\text{Se}$ and $\text{Cd}_{1-x}\text{Mn}_x\text{Se}$. This discrepancy cannot be eliminated, nor can it be improved, no matter how the fitting parameters $\omega_I(\text{MnSe:Zn})$ and $\omega_I(\text{ZnSe:Mn})$ are adjusted, within a reasonable range. We consider the reasons for the discrepancy as follows. In Peterson's method,⁴ the dependence of the force constant on the lattice parameter is given by

$$f(x) = F \left[1 + \theta \frac{a_{AC} - a(x)}{a_{AC}} \right], \quad (1)$$

where $a(x)$ and a_{AC} are the lattice parameters of mixed crystal $AB_{1-x}C_x$ and end member AC , respectively. F and θ are constants. Peterson assumed that the value of θ is the same for $\text{Cd}_{1-x}\text{Mn}_x\text{Te}$ and $\text{Zn}_{1-x}\text{Mn}_x\text{Te}$. If we, however, continue to use the assumption for $\text{Cd}_{1-x}\text{Mn}_x\text{Se}$ and $\text{Zn}_{1-x}\text{Mn}_x\text{Se}$, the static dielectric constant of MnSe calculated from the parameters in Table I would be $\epsilon_0(\text{MnSe}) = 1.38$. The value is too small and unreasonable as compared with usual II-VI compounds. This assumption seems then unsuitable for

TABLE I. Parameters in the MREI calculation (assuming same value of θ for $\text{Cd}_{1-x}\text{Mn}_x\text{Se}$ and $\text{Zn}_{1-x}\text{Mn}_x\text{Se}$). The parameters are from Ref. 9.

CdSe	ZnSe	MnSe
$\omega_{\text{TO}}(\text{CdSe}) = 171.5 \text{ cm}^{-1}$	$\omega_{\text{TO}}(\text{ZnSe}) = 205 \text{ cm}^{-1 \text{ a}}$	$\omega_{\text{TO}}(\text{MnSe}) = 219.5 \text{ cm}^{-1}$
$\omega_{\text{LO}}(\text{CdSe}) = 212.6 \text{ cm}^{-1}$	$\omega_{\text{LO}}(\text{ZnSe}) = 251 \text{ cm}^{-1 \text{ a}}$	$\omega_{\text{LO}}(\text{MnSe}) = 257 \text{ cm}^{-1}$
$\omega_I(\text{CdSe:Mn}) = 222.5 \text{ cm}^{-1}$	$\omega_I(\text{ZnSe:Mn}) = 234 \text{ cm}^{-1 \text{ *}}$	$\omega_I(\text{MnSe:Zn}) = 196.3 \text{ cm}^{-1 \text{ *}}$
$\epsilon_0(\text{CdSe}) = 9.53$	$\epsilon_0(\text{ZnSe}) = 8.80$	$\epsilon_0(\text{MnSe}) = 1.38 \text{ b}$
$a(\text{CdSe}) = 6.077 \text{ \AA}$	$a(\text{ZnSe}) = 5.670 \text{ \AA}$	$a(\text{MnSe}) = 5.902 \text{ \AA}$
Resultant force constants [$10^6 \text{ amu (cm}^{-1})^2$]		
$F_{\text{Cd-Se}} = 2.23$	$F_{\text{Zn-Se}} = 1.74$	$F_{\text{Mn-Se}} = 1.75$
$F_{\text{Cd-Mn}} = 1.41$	$F_{\text{Zn-Mn}} = 0.78$	

*Fitting parameters.

^aData from Ref. 6.

^bCalculated data.

$\text{Cd}_{1-x}\text{Mn}_x\text{Se}$ - $\text{Zn}_{1-x}\text{Mn}_x\text{Se}$ system. It can be understood by considering the implication of θ . θ describes the effect of variation of the lattice parameter on the force constants. Since the covalent radius of Zn (1.32 Å) and Cd (1.48 Å) are different, the effect of variation of the lattice parameter on force constants, i.e., the value of θ should be different for CdMnVI and ZnMnVI . This is more important in $\text{Cd}_{1-x}\text{Mn}_x\text{Se}$ - $\text{Zn}_{1-x}\text{Mn}_x\text{Se}$ than in $\text{Cd}_{1-x}\text{Mn}_x\text{Te}$ - $\text{Zn}_{1-x}\text{Mn}_x\text{Te}$ as the covalent radius of Se (1.16 Å) is smaller than Te (1.35 Å). In $\text{Cd}_{1-x}\text{Mn}_x\text{Se}$ and $\text{Zn}_{1-x}\text{Mn}_x\text{Se}$ the degree of variation of force constants with the lattice parameter is dominantly affected by the difference of Cd and Zn covalent radii, both having larger values than Se. In $\text{Cd}_{1-x}\text{Mn}_x\text{Te}$ - $\text{Zn}_{1-x}\text{Mn}_x\text{Te}$, however, due to the large covalent radius of Te, the difference of the variation of force constants between $\text{Cd}_{1-x}\text{Mn}_x\text{Te}$ and $\text{Zn}_{1-x}\text{Mn}_x\text{Te}$ is not so evident. This, as we believe, may account for why in Peterson's calculation the assumption of same value of θ for $\text{Cd}_{1-x}\text{Mn}_x\text{Te}$ and $\text{Zn}_{1-x}\text{Mn}_x\text{Te}$ still gives satisfying results.

Now we relax the constraint of same value of θ for $\text{Cd}_{1-x}\text{Mn}_x\text{Se}$ and $\text{Zn}_{1-x}\text{Mn}_x\text{Se}$. It allows us to select a reasonable value of $\epsilon_0(\text{MnSe})$, which we take as 10.0.¹² Then we calculate again the phonon frequencies of $\text{Zn}_{1-x}\text{Mn}_x\text{Se}$ as a function of composition with the parameters listed in Table II. The calculated curves are shown in Fig. 3 (left side). The resulted force constants are listed also in Table II. Those of $\text{Cd}_{1-x}\text{Mn}_x\text{Se}$ are calculated with the same method and shown in Fig. 3 (right side). Obviously the agreement between the experimental data and theoretical curves calculated by assuming different value of θ are much improved both in the zinc-blende range $\text{Zn}_{1-x}\text{Mn}_x\text{Se}$ and in $\text{Cd}_{1-x}\text{Mn}_x\text{Se}$.

There is still discrepancy between calculated curves and measured data in the wurtzite range $\text{Zn}_{1-x}\text{Mn}_x\text{Se}$ as Fig. 3 indicates. It is not surprising if one considers that the hexagonal crystal fields of wurtzite structure splits the F_2 vibrational modes of zinc-blende lattice into A_1 and E_1 modes, which are polarized along and perpendicular to the crystal axis \hat{c} , respectively.

Two facts are responsible for the splitting. One is the

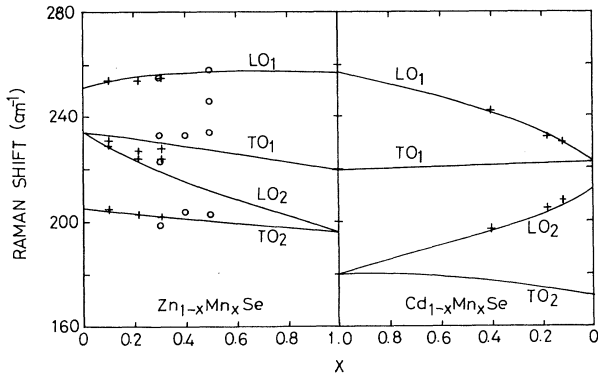


FIG. 3. The frequencies of the $\text{Cd}_{1-x}\text{Mn}_x\text{Se}$ and $\text{Zn}_{1-x}\text{Mn}_x\text{Se}$ zone-center optical phonons. The curves were generated using the MREI model assuming different values of θ for $\text{Cd}_{1-x}\text{Mn}_x\text{Se}$ and $\text{Zn}_{1-x}\text{Mn}_x\text{Se}$.

TABLE II. Parameters in the MREI calculation of $\text{Zn}_{1-x}\text{Mn}_x\text{Se}$ phonon frequencies (assuming different values of θ for $\text{Cd}_{1-x}\text{Mn}_x\text{Se}$ and $\text{Zn}_{1-x}\text{Mn}_x\text{Se}$). The parameters are from Ref. 9.

ZnSe	MnSe
$\omega_{\text{TO}}(\text{ZnSe})=205 \text{ cm}^{-1 \text{ a}}$	$\omega_{\text{TO}}(\text{MnSe})=219.5 \text{ cm}^{-1}$
$\omega_{\text{LO}}(\text{ZnSe})=251 \text{ cm}^{-1 \text{ a}}$	$\omega_{\text{LO}}(\text{MnSe})=257 \text{ cm}^{-1}$
$\omega_{\text{T}}(\text{ZnSe:Mn})=234 \text{ cm}^{-1 *}$	$\omega_{\text{T}}(\text{MnSe:Zn})=196.3 \text{ cm}^{-1 *}$
$\epsilon_0(\text{ZnSe})=8.80$	$\epsilon_0(\text{MnSe})=10.0$
$a(\text{ZnSe})=5.670 \text{ \AA}$	$a(\text{MnSe})=5.902 \text{ \AA}$
Resultant force constants [$10^6 \text{ amu} (\text{cm}^{-1})^2$].	
$F_{\text{Zn-Se}}=1.84$	$F_{\text{Mn-Se}}=2.02$
$F_{\text{Zn-Mn}}=0.67$	

*Fitting parameters.

^aData from Ref. 6.

local electric field E_{loc} which is given by¹³

$$E_{\text{loc}} = E + \left[\frac{4\pi}{3} + C_i \right] P \quad (2)$$

in wurtzite structure, where E and P are macroscopic field and polarization, respectively. C_i are constants and subscripts 1 and 2 represent its value for P parallel (A_1) and perpendicular (E_1) to \hat{c} , respectively. Veuleur and Barker¹³ have calculated C_i for an ideal wurtzite structure and got $C_1=0.2$, $C_2=-0.1$. The other is the crystal anisotropy in wurtzite structure, which results in the directional dependence of force constant and dielectric constant.

A complete method to describe the phonon mode in wurtzite structure with the MREI model requires the full calculation for A_1 and E_1 modes, respectively. However, for $\text{Zn}_{1-x}\text{Mn}_x\text{Se}$ the wurtzite structure exists within the range of $0.33 \leq x \leq 0.57$, thus no end member macroscopic parameters can be used to do such a calculation. We therefore adopt an alternative method to estimate the effect of the two facts mentioned above on phonon frequencies. We use Eq. (2) for wurtzite $\text{Zn}_{1-x}\text{Mn}_x\text{Se}$ and take $C_1=0.2$ and $C_2=-0.1$ for A_1 and E_1 modes, re-

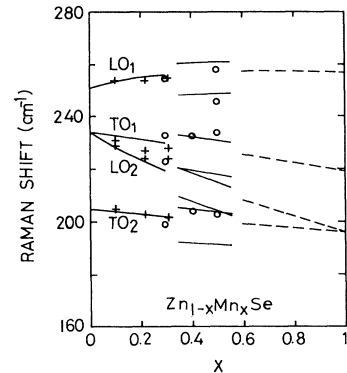


FIG. 4. The frequencies of the $\text{Zn}_{1-x}\text{Mn}_x\text{Se}$ zone-center optical phonons. Those curves are the same as Fig. 3 except that in the wurtzite structure directionally dependent force constants are used to describe the phonon-mode splitting.

spectively. Our calculation demonstrates a negligible splitting of A_1 and E_1 modes if only local field anisotropy is included. Such a small splitting does not agree with experimental data. Thus it seems necessary to consider another fact. To consider directionally dependent force constants in wurtzite structure we multiply the force constants resulted from the zinc-blende structure calculation by a factor f_i ($i=1$ for A_1 , $i=2$ for E_1). The values of f_i are determined by fitting calculated frequencies with the experiment results and are found to be $f_1=0.93$ and $f_2=1.03$. The curves generated using these directional-dependent force constants are illustrated in Fig. 4 (within the range $0.33 \leq x \leq 0.57$), which is in general agreement with experiment data. On the right side of Fig. 4 ($0.57 \leq x \leq 1$) we assume $Zn_{1-x}Mn_xSe$ exists in a hypothetical zinc-blende structure and the curves are represented by dashed lines.

CONCLUSION

Zone-center optical phonons in $Zn_{1-x}Mn_xSe$ exhibit intermediate-mode behavior. Generally speaking, the constant θ which describes the effect of the variation of the lattice parameter on the force constant should be different for different alloys. Once the structure is transformed from zinc blende to wurtzite, the optical-phonon modes in $Zn_{1-x}Mn_xSe$ are split due to crystal anisotropy. Using different force constants parallel and perpendicular to the \hat{c} axis a consistent description of both the theoretical calculation and experimental results is obtained.

ACKNOWLEDGMENT

The work at Fudan University received support by the National Natural Science Foundation Grant No. 68976007.

-
- ¹A. Anastassiadou, E. Liarokapis, and E. Anastassakis, *Solid State Commun.* **69**, 137 (1989).
²S. Venugopalan, A. Petrou, R. R. Gabizka, A. K. Ramdas, and S. Rodriguez, *Phys. Rev. B* **25**, 2681 (1982).
³R. G. Alonso, Y. K. Lee, E. Ch, and A. K. Ramdas, *Phys. Rev. B* **43**, 9610 (1987).
⁴P. L. Peterson, A. Petrou, W. Giriat, A. K. Ramdas, and S. Rodriguez, *Phys. Rev. B* **33**, 1160 (1986).
⁵R. D. Yoder-Short, U. Debska, and J. K. Furdyna, *J. Appl. Phys.* **58**, 4056 (1985).
⁶A. K. Arora, E. K. Suh, U. Debska, and A. K. Ramdas, *Phys. Rev. B* **37**, 2927 (1988).
⁷Lu Wei *et al.*, *Infrared Res. A* **7**, 425 (1988).
⁸W. Lu, P. L. Liu, G. L. Shi, S. C. Shen, and W. Giriat, *Phys. Rev. B* **39**, 1207 (1989).
⁹Y. S. Chen, W. Shockley, and G. L. Pearson, *Phys. Rev.* **151**, 648 (1966).
¹⁰I. F. Chang and S. S. Mitra, *Adv. Phys.* **20**, 359 (1971).
¹¹L. Genzel, T. P. Martin, and C. H. Perry, *Phys. Status Solidi B* **62**, 83 (1974).
¹²R. G. Alonso, E. K. Suh, A. K. Ramdas, N. Samarch, H. Luo, and J. K. Furdyna, *Phys. Rev. B* **40**, 3720 (1989).
¹³H. W. Verleur and A. S. Barker, *Phys. Rev.* **155**, 750 (1967).